Dynamical evolution of the Cybele asteroids

V Carruba, D. Nesvorný, Safwan Aljbaae, M E Huaman

Dynamical evolution of the Cybele asteroids

V. Carruba^{1*}, D. Nesvorný^2, S. Aljbaae^1, and M. E. Huaman^1
^{1} *UNESP, Univ. Estadual Paulista, Grupo de dinâmica Orbital e Planetologia, Guaratinguetá, SP, 12516-410, Brazil*
^{2} *Department of Space Studies, Southwest Research Institute, Boulder, CO, 80302, USA*

ABSTRACT

The Cybele region, located between the 2J:-1A and 5J:-3A mean-motion resonances, is adjacent and exterior to the asteroid main belt. An increasing density of three-body resonances makes the region between the Cybele and Hilda populations dynamically unstable, so that the Cybele zone could be considered the last outpost of an extended main belt. The presence of binary asteroids with large primaries and small secondaries suggested that asteroid families should be found in this region, but only relatively recently the first dynamical groups were identified in this area. Among these, the Sylvia group has been proposed to be one of the oldest families in the extended main belt.

In this work we identify families in the Cybele region in the context of the local dynamics and non-gravitational forces such as the Yarkovsky and stochastic YORP effects. We confirm the detection of the new Helga group at $\simeq 3.65$ AU, that could extend the outer boundary of the Cybele region up to the 5J:-3A mean-motion resonance. We obtain age estimates for the four families, Sylvia, Huberta, Ulla and Helga, currently detectable in the Cybele region, using Monte Carlo methods that include the effects of stochastic YORP and variability of the Solar luminosity. The Sylvia family should be $T = 1220 \pm 40$ Myr old, with a possible older secondary solution. Any collisional Cybele group formed prior to the late heavy bombardment would have been most likely completely dispersed in the jumping Jupiter scenario of planetary migration.

Key words: Minor planets, asteroids: general Minor planets, asteroids: individual: Cybele – celestial mechanics.

1 INTRODUCTION

The Cybele region, adjacent and exterior to the asteroid belt, is usually defined as the region in semi-major axis between the 2J:-1A and 5J:-3A mean-motion resonances with Jupiter. An increase in the number density of three-body resonances at semi-major axis larger than 3.7 (Gallardo 2014) makes the region between the Cybele area and the Hilda asteroids dynamically unstable, making the Cybele region the last outpost of an "extended" main belt, according to some authors (Carruba et al. 2013). Binary asteroids in the region suggested the presence of asteroid families, but only relatively recently a new dynamical family was found near 87 Sylvia (Vokrouhlický et al. 2010). The same authors suggested that 107 Camilla and 121 Hermione could have had families in the past that were dispersed by the local dynamics. The possibility that the Sylvia group might have been created just after the last phases of planetary migration, 3.8

Gyr ago, suggested by Vokrouhlický et al. (2010), may have interesting repercussions with regard to our understanding of the early Solar System history, and was one of the reasons why we started this research.

In this work we obtained dynamical groups in a newly identified domain of 1500 numbered and multi-opposition asteroids with high-quality synthetic proper elements, and revised the dynamical and physical properties. We then obtain age estimates of the four families identified in this work, Sylvia, Huberta, Ulla and Helga, with the method of Yarkovsky isolines and the Monte Carlo Yarko-Yorp approach of Vokrouhlický et al. (2006a, b, c). This method was modified to account for the stochastic YORP effect of Bottke et al. (2015), and historical changes of the Solar luminosity. Past and future dynamically evolution of present and past families is investigated using new symplectic integrators developed for this work. Finally, we analyzed the dynamical evolution of a fictitious Sylvia family formed before the late heavy bombardment in the jumping Jupiter scenario (Case I) of Nesvorný et al. (2013). We confirm the presence of the

* E-mail: vcarruba@feg.unesp.br

new Helga group (Vinogradova and Shor 2014) that could extend the boundary of the Cybele region up to the 5J:-3A mean-motion resonance, and the fact that the estimated age of the Sylvia could be compatible with an origin just prior to the late heavy bombardment. Families around 107 Camilla and 121 Hermione should disperse in timescales of the order of 1 Gyr, and could not be currently detectable.

This paper is so divided: in Sect. 2 we obtain synthetic proper elements for numbered and multi-opposition asteroids in the Cybele region, and review properties of mean-motion resonances in the area. In Sect. 3 we revise the role that secular dynamics play locally, and identify the population of asteroids currently in librating states of secular resonances. Sect. 4 deals with revising physical properties, when available, for local objects, while Sect. 5 discusses the problem of family identification, dynamical interlopers, and preliminary chronology using the method of Yarkovsky isolines. In Sect. 6 we obtain more refined estimates of the family ages and ejection velocities parameters using the Yarko-Yorp approach of Vokrouhlický et al. (2006a, b, c) modified to account for the stochastic YORP effect of Bottke et al. (2015), and variability of the Solar luminosity. Sect. 7 deals with investigating past and future dynamical evolution of present and (possibly) past families in the area using newly developed symplectic integrators that simulates both the stochastic YORP effect and variances in the past values of the Solar luminosity. Sect. 8 deals with the dynamical evolution of a fictitious Sylvia family formed before Jupiter jumped in the case I scenario of the jumping Jupiter model of Nesvorný et al. (2013). Finally, in Sect. 9, we present our conclusions.

2   PROPER ELEMENTS

We start our analysis by obtaining proper elements for asteroids in the Cybele region (defined as the region between the 2J:-1A and 5J:-3A mean-motion resonances with Jupiter, i.e., with an osculating semi-major axis between 3.28 and 3.70 AU). We computed synthetic proper elements for the 1507 numbered and 433 multi-opposition asteroids in the region, whose osculating elements were downloaded from the AstDyS site (http://hamilton.dm.unipi.it/astdys, Knežević and Milani 2003) on October 29th 2014, with the procedure discussed in Carruba (2010b). Of the 1940 particles, 1327 numbered asteroids and 317 multi-opposition survived for the length of the integration (10 Myr). We also eliminated all objects for which one of the proper elements $a, e, \sin(i)$ or proper frequencies g and s had errors larger than those classified as "pathological" by Knežević and Milani (2003); i.e., $\Delta a = 0.01$ AU, $\Delta e = 0.1$, $\Delta \sin(i) = 0.03$, and $\Delta g = \Delta s = 10 \ arc-sec \cdot yr^{-1}$. This left us with a data-set of 1225 numbered and 275 multi-opposition asteroids with proper elements in the orbital region, for a total of 1500 asteroids with good-quality proper elements.

A projection in the $(a, sin(i))$ plane of the proper elements (with their errors in proper a) for the surviving 1500 objects is shown in Fig. 1. Objects classified as having unstable proper a ($0.0003 < \Delta a < 0.01$ AU) are shown as yellow full dots. We then computed the location of two- and three-body mean-motion resonances with the approach of Gallardo (2014). This method allows to compute the value of
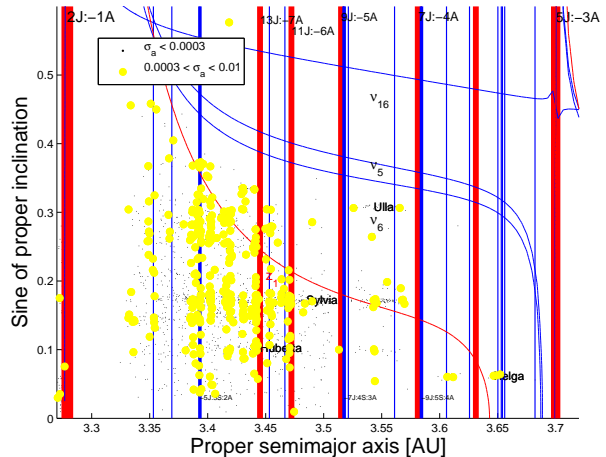

Figure 1. An $(a, \sin i)$ projection of proper elements for numbered and multi-opposition asteroids in the Cybele region.

the semi-major axis of the resonance center and to estimate the resonance strength through a parameter R_S whose maximum value is one. The location of three-body resonances was estimated up to order 30 including planets from Earth to Uranus, and using the values of eccentricity, inclination and argument of pericenter of 87 Sylvia, the asteroid with the largest family in the region. Two-body resonances with R_S up to 10^{-5} and three-body mean-motion resonances with R_S up to 10^{-4} are shown as vertical red lines and blue lines, respectively (for simplicity we only identify three-body resonances with $R_S > 5 \cdot 10^{-2}$. The thickness of the lines is associated with the resonance strength. Linear secular resonances are displayed as blue lines, while the inclined red line display the approximate location of the center of the z_1 non-linear secular resonance (see Carruba (2010b) for a description of the method used to plot the center of libration for secular resonances). The names of the asteroid families discussed in Nesvorný et al. (2015) and the Helga family of Vinogradova and Shor (2014) are also shown in the figure.

Most of the objects with unstable values of proper a are perturbed by two and three-body resonances such as the 13J:-7A, 11J:-6A, and -5J:3S:2A. As observed by several other authors (Milani and Nobili 1985, Vokrouhlický et al. 2010), known asteroid families tend to cluster in the regions with lower number density of resonances. If we define highly inclined asteroids as those with inclination higher than that of the center of the ν_6 secular resonance, only one numbered asteroid satisfies this criteria: 1373 Cincinnati, with an inclination of 38.97°. Generally speaking, the ν_6 secular resonance forms the upper boundary in inclination of the Cybele region, while the 2J:-1A and 4J:-7A mean-motion resonances with Jupiter delimit the region in semi-major axis for most of the asteroids in the region, with the notable exception of the new (522) Helga group, between the 4J:-7A and 5J:-3A mean-motion resonances, that could be the main belt family most distant from the Sun (Vinogradova and Shor 2014), and is of particular interest because of the very peculiar dynamics of 522 Helga, characterized by weak instabilities on extremely long timescales, the so-called "stable chaos" of Milani and Nobili (1992, 1993). Asteroids in the Cybele region do not generally experience planetary close encounters. The region is also crossed by a web of non-linear secular

resonances, of which the most studied (Vokrouhlický et al. 2010) is the $z_1 = \nu_6 - \nu_{16} = g - g_6 + s - s_6$ secular resonance. We will further discuss secular dynamics in the region in the next section.

3 SECULAR DYNAMICS IN THE CYBELE REGION

Secular resonances occur when there is a commensurability between the proper frequency of precession of the argument of pericenter g or of the longitude of the node s of a given asteroid and a planet. If the commensurability is just between one frequency of the asteroid and one frequency of the planet, such as in the case of the $\nu_6 = g - g_6$ secular resonance, the resonance is linear. Higher order resonances involving more complex combinations of asteroidal and planetary frequencies, such for instance the $z_1 = \nu_6 + \nu_{16} = g - g_6 + s - s_6$ resonance, are called non-linear secular resonances. Carruba (2009a) defines as likely resonators the asteroids whose frequency combination is to within ± 0.3 arcsec/yr from the resonance center. For the case of the z_1 resonance, this means that $g + s = g_6 + s_6 = 1.898$ arcsec/yr. About 90% of the z_1 likely resonators in the Padua family area were found to be actual librators, when the resonant argument of the resonance was analyzed.

We selected likely resonators for all non-linear secular resonances in the Cybele region up to order six following the procedure described in Carruba et al. (2013), and then verified that the appropriate resonant argument for each of these asteroids was in a librating state. Fig. 2 displays a projection in the proper $(g, g + s)$ plane of asteroids in the region (panel A), as well as a projection of asteroids found to be in librating states of non-linear secular resonances in the region (panel B, only two-body resonances were reported in this plot for simplicity). Our results are summarized in Table 1, where we display the name of the resonances with a population of asteroids larger than 1, the value of the combination of planetary frequencies in the resonant argument, the number of likely resonators, and the number of asteroids actually found in librating states.

No asteroids in the Cybele region were found to be in or near linear secular resonances. The large number of likely resonators found for the $2\nu_6 - \nu_5$ resonance is in fact an artifact caused by the perturbation on the g frequency value of objects near the separatrix of the 2J:-1A mean-motion resonance (no asteroid was found to be in librating states of this resonance by our analysis). Three $g + s$ resonances have the largest population of librators, the z_1 resonance with 22 asteroids (most of which are found in or near the Sylvia family (Vokrouhlický et al. 2010)), the $\nu_5 + \nu_{16}$ (six bodies), and the $2\nu_6 - \nu_5 + \nu_{16}$ with five objects. Other local non-linear resonances with populations of librators of just one object were not listed for the sake of brevity.

Having revised the effect of local dynamics, we are now ready to analysis the taxonomical properties of asteroids in the Cybele region.

Table 1. Main secular resonances in the Cybele region, frequency value, number of likely and actually resonant asteroids.

Resonance argument	Frequency value ["/yr]	Likely resonators	Actual resonators
g resonances			
$2\nu_6 - \nu_5$	52.229	44	0
g+s resonances			
$\nu_5 + \nu_{16}$	-22.088	6	6
$\nu_6 + \nu_{16}$	1.898	29	22
$2\nu_6 - \nu_5 + \nu_{16}$	25.884	8	5
g+2s resonances			
$\nu_5 + 2\nu_{16}$	-48.433	3	0

4 COMPOSITIONAL ANALYSIS: TAXONOMY, SDSS-MOC4, AND WISE DATA

In this section we will follow the same approach used by Carruba et al. (2014b) in their analysis of the Euphrosyne family. A more in depth description of the methods used can be found in that paper. Only three objects had taxonomical data in three major photometric/spectroscopic surveys (ECAS, SMASS, and S3OS2, see references in Carruba et al. 2014b): 692 Hippodamia (S-type), 522 Helga, and 1373 Cincinnati (X-types). Using the classification method of De Meo and Carry (2013) that employs Sloan Digital Sky Survey-Moving Object Catalog data, fourth release (SDSS-MOC4 hereafter, Ivezic et al. 2001) to compute gri slope and $z' - i'$ colors, we obtained a set of 238 observations of asteroids (including multiple observations of the same object) in the Cybele region. This corresponds to 118 asteroids for which a SDSS-MOC4 taxonomical classification and proper elements are both available. We found 44 X-types, 41 D-types, 23 C-types, 5 L- and S-types, and one A- and B-type object, respectively.

Fig. 3, panel A, displays a projection in the gri slope versus $z - i$ plane for the 238 observations in the SDSS-MOC4 catalogue for asteroids in the Cybele region, while panel B shows an $(a, sin(i))$ projection of asteroids in the same region. As in Carruba et al. (2013), we found that the Cybele region is dominated by dark, primitive objects, with a sizeable fraction of D-type bodies that were not identifiable with the methods used in Carruba et al. (2013). The Sylvia family seems to be compatible with a CX-complex taxonomy. The primitive, dark nature of most objects in the region is confirmed by an analysis of the values of geometric albedos from the WISE mission (Masiero et al. 2012). We identified 568 asteroids with WISE albedo information in the Cybele region. Our analysis confirms that of Carruba et al. (2013) (see Fig. 15): the vast majority of bodies in the Cybele region has low albedos ($p_V < 0.15$), with only
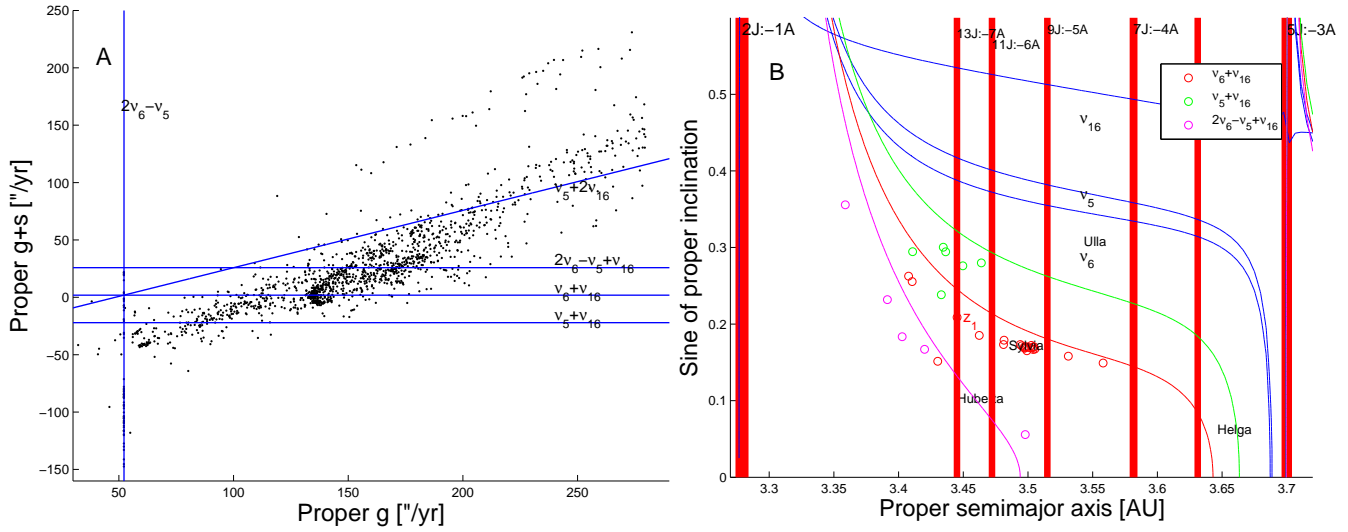
Figure 2. Panel A: a (g,g+s) projection of the 1485 asteroids with known proper elements in our sample. Blue lines identify the location of the secular resonances listed in Table 1 with a population of "likely resonators" larger than 1. Panel B: an (a,sin(I)) projection of the actual resonators population listed in table 1.
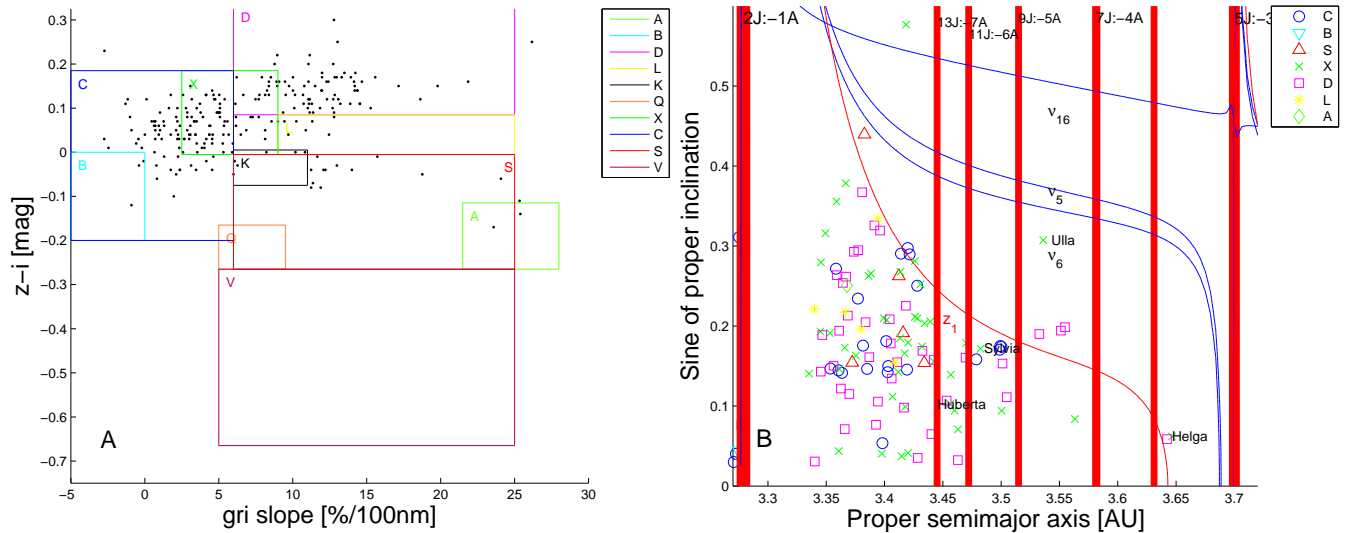

Figure 3. Panel A: a projection in the gri slope versus z-i plane of the 238 observations in the SDSS-MOC4 catalogue for asteroids in the Cybele region. Panel B: an $(a, sin(i))$ projection of asteroids with taxonomical type in the same area.

11 asteroids with intermediate values $(0.15 < p_V < 0.3)$, and one single bright object with $p_V > 0.3$. Using the values of the diameters from WISE, when available (otherwise diameters are estimated using absolute magnitudes and the mean value of geometric albedo in the Cybele region, i.e., $p_V = 0.067$ via Eq. 4 in Carruba et al. 2003), and the density of 87 Sylvia from Carry (2012), we computed the masses of asteroids in the Cybele region, assumed as homogeneous spheres. For the few asteroids where an estimate of the mass was reported in Carry (2012), we used the values from that paper.

Fig. 4 shows an $(a, sin(i))$ projection of the family members, where the sizes of the dots are displayed according to the asteroid masses. Of the four asteroids with masses larger than 10^{19} kg, 65 Cybele, 87 Sylvia, 107 Camilla, and 420 Bertholda, only 87 Sylvia is currently associated with

a dynamical family. Vokrouhlický et al. (2010) suggested the possibility that 107 Camilla and 121 Hermione, both of which are large binary asteroids, supposedly generated during collisionary events, could have possessed family in the past that were dispersed through a combination of diffusion via the Yarkovsky effect and numerous weak resonances over timescales of a Gyr. We will further investigate this hypothesis later on in this paper.

Having now revised physical and taxonomical properties of local asteroids, in the next section we will start identifying dynamical groups in the region.
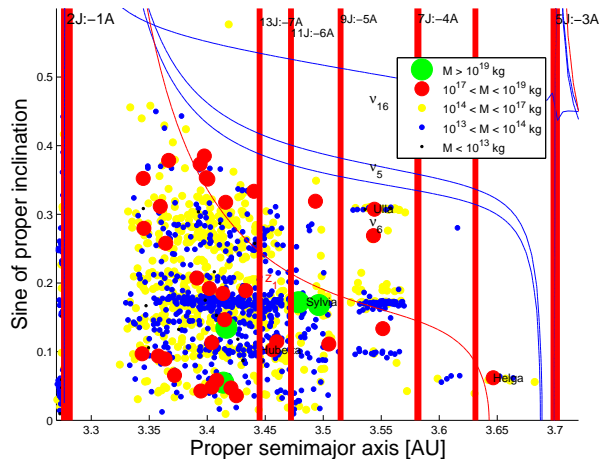
Figure 4. An $(a, sin(i))$ projection of the asteroids in the Cybele region. The sizes of the dots are proportional to the asteroid masses, according to the color code in the figure legend.

5   FAMILY IDENTIFICATION

Several papers have discussed how to identify asteroid families using the hierarchical Clustering method (HCM). Here we follow the approach of Carruba (2010b), see also Zappalá et al. (1995) for a discussion the HCM. Key parameters of the HCM are the nominal distance velocity cutoff for which two nearby asteroids are considered to be related and possibly part of the same family, and the minimal number of bodies for having a statistically significant family. Using the approach of Beaugé and Roig (2001) we found for our sample of 1500 asteroids with proper elements in the Cybele region a nominal distance velocity cutoff of 138.2 m/s, and a minimal family number of 25.

We constructed a stalactite diagram for asteroids in the region using the approach of (Zappalà et al. 1990). We selected (87) Sylvia, the largest body of the most numerous family in the region, and used a value of the cutoff large enough that almost all Cybele asteroids were considered part of the family. We then lowered the value of the cutoff and checked if new dynamical groups appeared among the asteroids no longer connected to the Sylvia family.

Fig. 5 displays our results. Asteroids belonging to a family are identified by black dots, the horizontal red line shows the value of the nominal distance velocity cutoff as obtained with the Beaugé and Roig (2001) approach. At this value of nominal cutoff only the three robust families of Nesvorný et al. (2015) are detectable: 87 Sylvia (FIN 603, where FIN is the Family Identification Number, as defined in Nesvorný et al. 2015), 260 Huberta (just a candidate family in Nesvorný et al. 2015), and 909 Ulla (FIN 903). The smaller family around 45637 2000 EW12, reported in Milani et al. (2014), disappears for smaller cutoffs and merges with the Sylvia family for higher cutoffs, and will not be considered as robust in this work. Of the new families proposed by Vinogradova and Shor (2014), we were able to only confirm the group around 522 Helga, and for the larger value of the cutoff of 180 m/s (this larger value is justified by the fact that these asteroids are found in a emptier region, with higher values of the mean distances among bodies with respect to the Cybele region). The proposed family of

Table 2. Proper element based families in the Cybele region.

Name	N	N_{SDSS}	N_{WISE}	Interlopers	Max. age [Myr]
87 Sylvia	363	12	99	8	3800
260 Huberta	56	4	24	8	3000
522 Helga	12	2	1	0	800
909 Ulla	30	1	14	2	1200

643 Scheherezade, associated in our work with asteroid 1556 Wingolfia, disappears for cutoffs of 200 m/s, and we could not identify in this paper the proposed groups around 121 Hermione, 1028 Lydina, and 3141 Buchar. We could also not positively identify the "rump" families around 107 Camilla and 121 Hermione proposed by Vokrouhlický et al. (2010). In that work the authors suggested that the original families around these bodies, all large asteroids with small satellites at large separations, configuration that could be the result of the formation of a collisional family, could have possibly been lost because of interaction with the local dynamics in timescales of Gyr, and that, possibly, only "rump" families made by the largest remnants could have yet be found near these asteroids. We did not identified any cluster near Hermione, and this asteroid merged with the Huberta family at a 200 m/s level. There was a small clump of 16 asteroids near Camilla at 110 m/s, but apart from four asteroids and Camilla itself that had diameters larger than 5 km, the other objects are too small to have possibly survived 4 Gyr of dynamical evolution. The possible existence of rump families near these asteroids remains, therefore, yet to be proved, in our opinion. Finally, the Sylvia family breaks down into four minor groups at cutoffs of 100 m/s or lower.[1].

Our results are summarized in Table 2, that reports the smallest numbered family member, the number of asteroids in the group, and those with data in the SDSS-MOC4 and WISE database. There were 12 asteroids with SDSS colors in the Sylvia family, 4 in the Huberta, 2 in the Helga, and one in the Ulla group. All these objects are dark, primitive asteroids belonging to the C-, X-, and D-classes, and the WISE albedo data is also compatible with this scenario, since all family members with values of geometric albedos are dark bodies with $p_V < 0.15$. Fig. 5, panel B, displays the orbital locations of our confirmed four families, shown as colored dots, superimposed to contour plots of number density of asteroids in the Cybele region. We computed the

---

[1]   As in Carruba (2010b) we also searched for asteroid pairs in the region. These objects, extremely close in proper element space, could either be associated with double or multiple asteroid systems that recently separated, or be fragments launched by impacts onto very similar orbits (Pravec and Vokrouhlický 2009). The first two pairs with mutual distances less than 7.0 m/s were 113317 (2002 RL200) and 2007 RW290, and 216212 (2006 UC73) and 239503 (2007 VH165) .
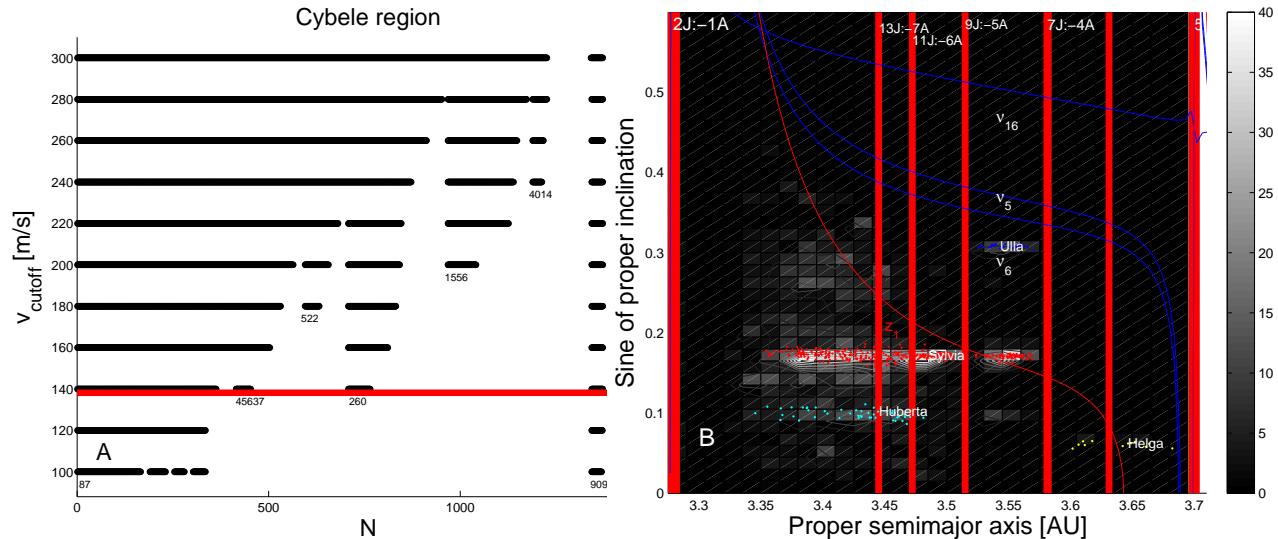
Figure 5. Panel A: stalactite diagram for the 1500 asteroids in the Cybele region. Asteroids belonging to a family are identified by a black dots. Panel B: contour plot of number density of asteroids in the same region. Colored dots show the location of members of the four identified asteroid families.

number of asteroids per unit square in a 30 by 42 grid in the $(a, sin(i))$ plane, with a between 3.26 and 3.70 and $sin(i)$ between 0.00 and 0.63. Three inclination regions of higher asteroidal number density can be identified in the map: one around $sin(i) \simeq 0.3$, associated with the Vinogradova and Shor (2014) Scheherezade family, one at $sin(i) \simeq 0.18$, occupied by the Sylvia family, and one at $sin(i) \simeq 0.1$, associated with the Huberta group. The other minor local higher density regions are occupied by the Ulla and Helga families.

As a next step in our analysis we obtain a preliminary estimate of the age of the families and to eliminate possible dynamical interlopers using the method of Yarkovsky isolines. In this approach first the barycenter of the family is computed using the estimated diameters from WISE (when available), and values of the density of the main family objects from Carry (2012). Then isolines of displacements caused by the Yarkovsky effects for objects starting at the family barycenter are computed for different estimated family ages, using values of the parameters describing the Yarkovsky force from Brož et al. (2013), Table 2. For families older than 2000 Myr we also accounted for diffusion caused by close encounters with massive asteroids, estimated to be of the order of 0.02 AU over 4 Gyr. Dynamical interlopers are objects that reside beyond the maximum possible Yarkovsky isoline, and could not have reached their current orbital position since the family formation. A more in depth description of this method is available in Carruba et al. (2014b).

Fig. 6 displays the results of our method for the Sylvia family, the largest group in the Cybele region. We computed Yarkovsky (plus close encounters) isolines for 2.5 Gyr, the estimated age of the family according to Vokrouhlický et al. (2010), and for 3.8 Gyr, the estimated age of the Late Heavy Bombardment (LHB) according to Brož et al. (2013). Our results for this and other families in the area are summarized in Table 2, columns 5 and 6, where we report the number of dynamical interlopers and the estimated maximum age for each given family. We found 8 dynamical interlopers (aster-
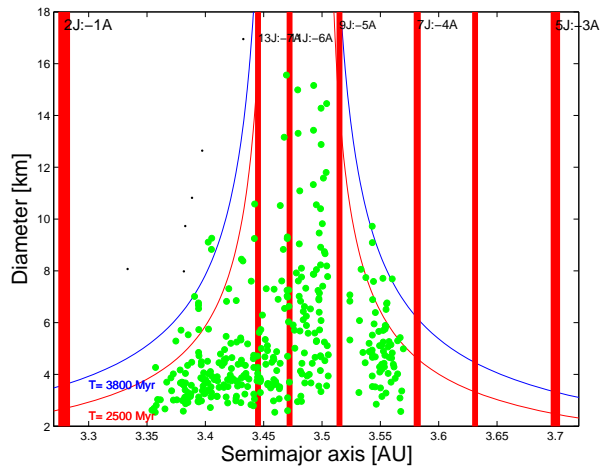

Figure 6. A proper a versus radius projection of members of the Sylvia family. The red and blue curves displays isolines of maximum displacement in a caused by Yarkovsky effect and close encounters with massive asteroids computed from the family barycenter after 2.5 Gyr (red line) and 3.8 Gyr (blue line). Green full dots are associated with Sylvia family members, black dots display the location of dynamical interlopers.

oids 107, 5914, 9552, 11440, 12003, 63050, 111526, 133402, 167625) in the Sylvia family, 8 (401, 3622, 4003, 5362, 7710, 13890, 14330, 77837) in the Huberta group, and 2 (60042, 114552) in the Ulla family. The Sylvia family could be one of the few groups created during the LHB, and the Huberta family is characterized by an asymmetry between lower and higher semi-major axis asteroids, with a larger fraction of the family closer to the Sun (the estimate of the age significantly decreases if we disconsider a larger fraction of the members closer to the Sun). The Ulla and Helga groups have relatively small populations of members (29 and 12, respectively), which undermines the possibility of obtaining more precise estimates of these groups ages. In the next section

we will use the so-called Yarko-Yorp Monte Carlo method of Vokrouhlický et al. (2006a, b, c), modified to account for new developments in our understanding of the YORP effect, to try to refine the preliminary estimates of the family ages obtained in this section.

6 CHRONOLOGY

Monte Carlo approach to obtain estimates of the family age and ejection velocity parameters were pioneered by Vokrouhlický et al. (2006a, b, c) for the Eos and other asteroid groups. Here we modified that method to also account for the stochastic version of the YORP effect, as modeled by Bottke et al. (2015). To account for the effect of shape changes on the torques acting on a given asteroid during YORP cycles, recently Bottke et al. (2015) introduced the so-called "stochastic YORP" model. In this model, a different torque solution is chosen every time the τ_{YORP} timescale (of the order of 1 Myr) is exceeded. This approach changes the evolution of the asteroid periods with respect to the "static YORP" effect in which shapes remained fixed between YORP cycles, but does not affect the time-behavior of the asteroid obliquities, which are still driven toward the end states of $0°$ and $180°$. To estimate the age and other parameters of the given asteroid family, basically, first the (a, H) values of asteroids are mapped into a C-parameter using the relationship:

$$0.2H = log_{10}(\Delta a/C). \tag{1}$$

Then, fictitious distributions of asteroids for different values of the ejection velocity (and other) parameters are evolved under the influence of the Yarkovsky effect, both diurnal and seasonal versions, the YORP effect, and, in some cases, the long-term effect of close encounters with massive asteroids (Carruba et al. 2014a). Changes in the angular rotation velocity ω and spin obliquity (the inclination of the spin axis with respect to the normal to the orbital plane of the asteroid) ϵ caused by the YORP effect are computed by solving the system of differential equations:

$$\omega\frac{d\epsilon}{dt} = g(\epsilon) \tag{2}$$
$$\frac{d\omega}{dt} = f(\epsilon), \tag{3}$$

where the $g-$ and $f-$ functions are displayed in Fig. 7 (see also Bottke et al. 2015). These functions were computed for a $D = 2$ km body at $a = 2.5$ AU, with a bulk density of $\rho_{bulk} = 2500$ kg/m^3 and a period of 8 hrs. The strength of the YORP effect is proportional to $1/(\rho_{bulk}a^2D^2)$. The gray zone in the figure in between the blue lines displays the variance of the results for various asteroidal shapes in Čapek and Vokrouhlický (2004). The full and dotted lines show the behavior of solution for accelerating and decelerating bodies, respectively. While in the so-called static YORP the $f-$ and $g-$ functions are constant between end states of the YORP cycle, in the stochastic YORP, to account for the changes in the shape of the asteroid produced by increasing or decreasing spin periods, these two functions are randomly changed on time-scale of 1 Myr (see Bottke et al. 2015 for more details on the modeling of this effect). Once a C-target

values distribution has been obtained for test particles subjected to the Yarkovsky, YORP, and, possibly, other force, the real and fictitious distributions of C-target values are then compared using a χ^2-like variable $\psi_{\Delta C}$ (Vokrouhlický et al. 2006a, b, c), whose minimum value is associated with the best-fitted solution.

Of the four families identified in this work, only the Sylvia and (barely) the Huberta group have enough members to have a distribution of C-target values large enough for the method to be appliable. We will start our analysis by investigating the Sylvia group.

6.1 Sylvia family

As discussed in Sect. 5, the Sylvia family may be as old as 4.2 Gyr. Since in the past the solar luminosity was weaker, and this affects the strength of the Yarkovsky force, following the approach of Vohkroulický et al. (2006a) we modified the Yarko-Yorp code to also account for older values of the solar luminosity $L(t)$ given by the relationship:

$$L(t) = L_0\left[1 + 0.3\left(1 - \frac{t}{t_0}\right)\right]^{-1}, \tag{4}$$

where L_0 is the current value of the solar constant ($1.368 \cdot 10^3 W/m^2$), $t_0 \simeq 4.57$ Gyr is the age of the Sun, and t is the time measured from the Solar System formation. We then computed values of the χ^2-like parameter for 28 values of the ejection velocity parameter V_{EJ} up to 140 m/s (the current escape velocity from 87 Sylvia is 111.74 m/s, values of V_{EJ} higher than the escape velocity were not likely to occur, according to Bottke et al. 2015), using values of the Yarkovsky parameters (and other parameters needed by the Yarko-Yorp model such as C_{Yorp}, $c_{reorient}$ and δ_{YORP} whose descriptions and used values can be found in Bottke et al. 2015), already discussed in previous sections and typical of C-complex families as Sylvia (see also Table 2 of Brož et al. 2013).

As in previous papers, to avoid problems caused by possible fluctuations in the $N(C)$ distribution, we also computed an average C distribution for the family obtained as a mean of C distributions, each corresponding to five values of a_c (in the range [3.4785, 3.4789] AU, near the family barycenter). To avoid the problem of small divisors, we did not considered 3 intervals in C with less than 3 asteroids (about 1% of the total population of 354), leaving us with a total of 25 intervals in C.

Fig. 8 displays our results. As discussed in Vokrouhlický et al. (2006a), the estimated age of the family is about 10% older when the effect of lower past solar luminosities is accounted for. For values of V_{EJ} lower than the escape velocity from 87 Sylvia, we found two minima, one (red curve in Fig. 8) for $T = 1220^{+40}_{-40}$ Myr and $V_{EJ} = 95^{+13}_{-3}$ m/s, for $\psi_{\Delta C} = 24.5$, corresponding at a confidence level of 56.7% of the two distribution being compatible (Press et al. 2001), and a much weaker one (blue curve) for $T = 4220^{+100}_{-120}$ Myr and $V_{EJ} = 35^{+45}_{-15}$ m/s, for $\psi_{\Delta C} = 58.5$, corresponding at a confidence level of just 0.8%. The possible existence of two distinct minima may either suggests that i) the Sylvia family could be the result of two distinct cratering events, with the less likely solution corresponding to an older cratering event, or ii) the secondary solution is just a statistical fluke.
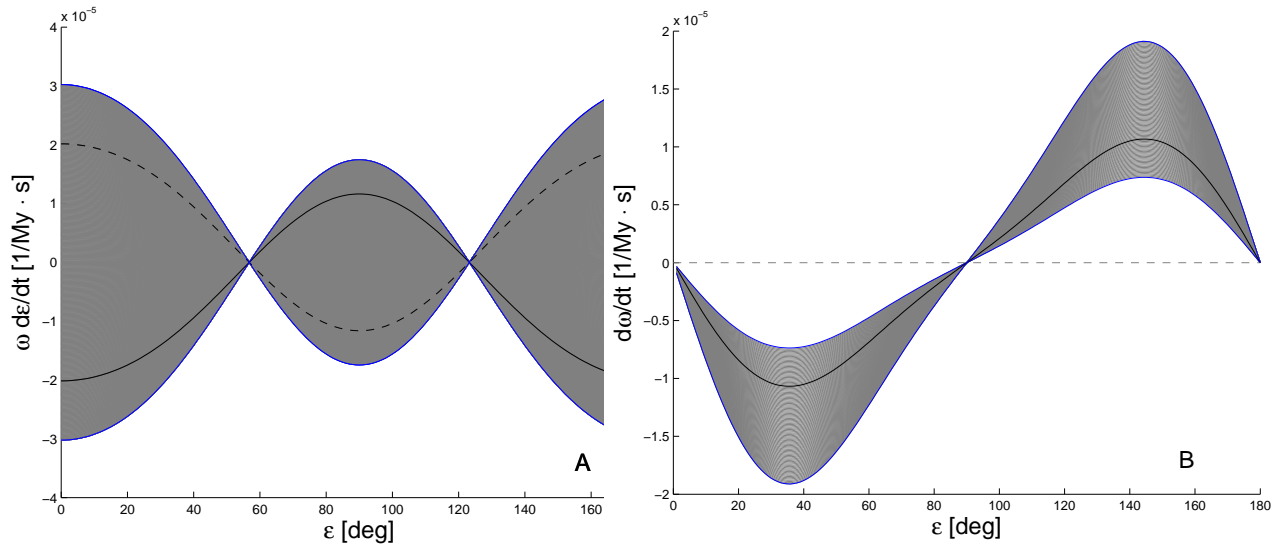
Figure 7. Dependence of the $g-$ (panel A) and $f-$ (panel B) functions on the spin obliquity ϵ. Panel A displays $g = \omega(d\epsilon/dt)$, while in panel B we show $f = d\omega/dt$. Blue lines display the curves of maximum variance of the $f-$ and $g-$ functions, while the gray zone is associated with the variance of the results. The full and dotted lines show the behavior of solution for accelerating and decelerating bodies, respectively.
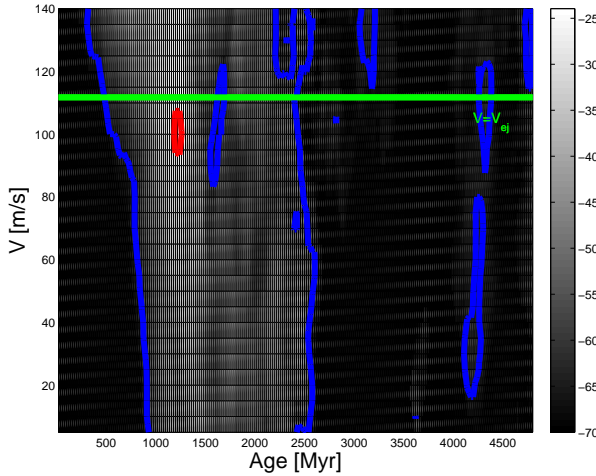

Figure 8. Target function $\psi_{\Delta C}$ values in the (Age, V_{EJ}) plane for Sylvia families simulated with the stochastic Yarko-YORP Monte Carlo model, modified to account for lower solar luminosity in the past. The red and blue lines identify the values of the target function associated with the two given probabilities of the simulated distribution agreeing with the real one. The horizontal green line shows the value of the ejection velocity from 87 Sylvia.

Figure 9. Target function $\psi_{\Delta C}$ values in the (Age, V_{EJ}) plane for Huberta families simulated with the same approach used for the Sylvia family.

We will further investigate these two scenarios in the next section.

6.2   Huberta family

After eliminating the dynamical interloper, the Huberta family still possessed 48 members. We created a C-target function distribution with 9 intervals in C equally spaced by $\Delta C = 20 \cdot 10^{-6}$ and starting at $C = -9 \cdot 10^{-5}$. Again, we used five values of a_c near the family barycenter to compute the distribution of $N_{obs}(C)$, that was then averaged among the five values. The escape velocity from 260 Huberta is
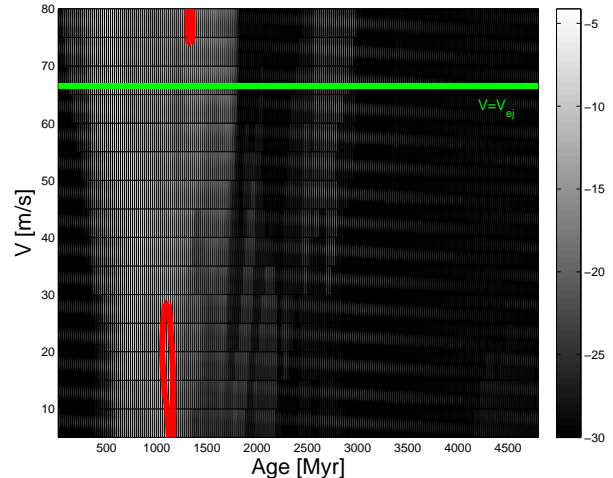
66.5 m/s (displayed as a horizontal green line in Fig. 9), we expect therefore that the best-fitted solution should have values of V_{EJ} lower than that.

Fig. 9 displays our results: we found a minimum for $T = 1100 \pm 50\ Myr$ and $V_{EJ} = 15^{+13}_{-15}$ m/s, at a confidence level of 91.8%. We did not identify significant secondary minima for the Huberta family. The dynamical evolution of this and other families in the Cybele region will be further investigated in the next section.
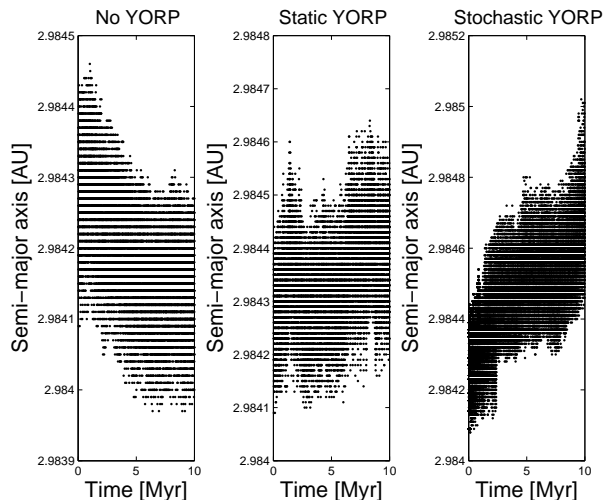
Figure 10. Time evolution of the osculating semi-major axis of a particle integrated under the effect of the Yarkovsky effect and no YORP force (left panel), under the static YORP effect (central panel), and under stochastic YORP (right panel).

7 DYNAMICAL EVOLUTION OF FAMILIES IN THE CYBELE REGION

7.1 Future dynamical evolution

To further investigate the dynamical evolution of dynamical groups in the Cybele region, we performed numerical integration with the $SWIFT - RMVSY$ integrator of Brož (1999), able to model the diurnal and seasonal Yarkovsky force and the effect of close encounters of massless particles with massive planets, and with the new $SYSYCE$ integrator (Swift+Yarkovsky+Stochastic Yorp+Close encounters), that modifies the São Paulo integrator of Carruba et al. (2007), a code that modeled the Yarkovsky force and close encounters of massless particles with massive bodies, to also include the stochastic YORP effect, as described in Bottke et al. (2015). For completeness, we also modified $SWIFT$-$RMVSY$, so as to account for both the static and stochastic versions of the YORP effect. While we do not consider the long-term effect of close encounters with massive asteroids in this work, the $SYSYCE$ integrator can in principle also account for this perturbation.

Fig. 10 displays the time evolution of the osculating semi-major axis of a test particle in the Euphrosyne family region integrated over 10 Myr under the gravitational effect of all planets and (31) Euphrosyne[2], with the São Paulo integrator (No YORP, left panel); using the new integrator including the static version of the YORP effect (Static YORP, central panel); and using the new integrator while including the stochastic YORP effect (Stochastic YORP, right panel). For our runs, we used the optimal values of the Yarkovsky parameters discussed in Brož et al. (2013) for C-type asteroids. The initial spin obliquity was 0° for the simulation without the YORP effect and random in the other two cases. Normal reorientation timescales due to possible collisions as described in Brož (1999) were considered for all runs. As can

Table 3. Time needed for the family to have less than 8 members (dispersion time) for simulations with the $SWIFT - RMVSY$ and $SYSYCE$ integrators.

Family	Dispersion time $SWIFT - RMVSY$ [Myr]	Dispersion time $SYSYCE$ [Myr]
Sylvia	2650	4020
Huberta	1650	2270
Ulla	650	705
Helga	305	320

be seen in the figure, the particle experienced just a single event of reorientation at about 1 Myr, and then evolved under the Yarkovsky force with a retrograde obliquity, toward smaller values of semi-major axis. In the simulation with the static YORP integration, reorientations occurred twice, once because of a collision (at about 1 Myr), and once because the period of the test particle reached a limit value (2 or 1000 hrs, see Bottke et al. 2015 for a discussion of what happens at the YORP cycle end-states), at about 3 Myr. As a consequence, the test particle started evolving toward larger values of a, then reoriented its spin axis and evolved toward smaller a values, and finally reoriented once again and evolved toward larger values of a. More interesting was the case of the stochastic YORP integration. Here the shape of the test particle (but not its orientation) was changed every Myr. As a consequence, the test particle underwent a less severe random walk, tending to generally increase its semi-major axis over the integration. Similar behavior was observed for several other test runs performed with the new symplectic code. Results for simulations with the modified versions of the $SWIFT$-$RMVSY$ integrator are compatible, within numerical errors, with that of the SYSYCE integrators, for both the static and stochastic version of the YORP force.

Having tested the new integrator, for our runs with Cybele asteroids again we used the optimal values of the Yarkovsky parameters discussed in Brož et al. (2013). Normal reorientations timescales due to possible collisions, as described in Brož (1999), were considered for all runs with the $SYSYCE$ integrator, but not for those with $SWIFT - RMVSY$, so as to obtain the maximum possible drift rates for these simulations. All particles were subjected to the gravitational influence of all planets. For the simulations with $SWIFT - RMVSY$ we used for each family member, as determined in Sect. 5, two sets of orbital obliquity, 0° and 180°, so as to maximize the strength of the Yarkovsky force. Random spin obliquities were assigned to the test particles for the simulations with the $SYSYCE$ integrator. We integrated our test particles over 4.0 Gyr, under the influence of all planets.

We first obtained synthetic proper elements for our test particles with the methods described in Sect. 2 and computed the number of particles that remained in the four studied family regions, defined as boxes in the $(a, e, sin(i))$ domain delimited by the maximum and minimum value of
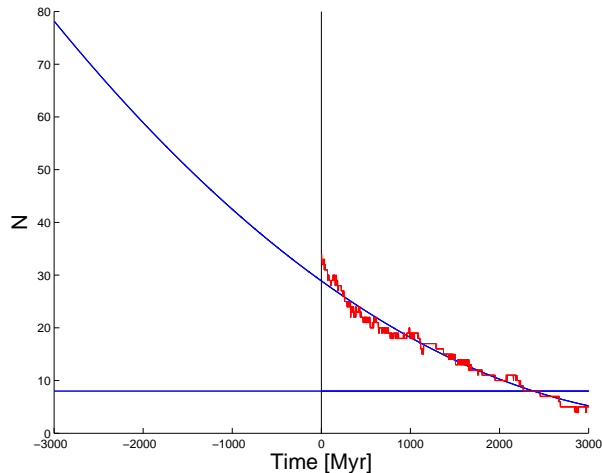
---

[2] The mass of (31) Euphrosyne ($M = 1.27 \pm 0.65 \cdot 10^{19}\ kg$) was taken from Carry (2012).

Figure 11. Number of simulated asteroids in the Huberta family region as a function of time (red line). The blue line displays results of a best-fitted second order polynomial to the $(time, N)$ function extended to the maximum possible age of the Huberta family (3 Gyr). The vertical black line displays present time, and the horizontal blue line the minimum number of asteroid needed to recognize the family as a clump (8).

Table 4. Dispersion times for results of past dynamical evolution of families in the region.

Family	Initial time [Myr]	Dispersion time [Myr]
Sylvia	4200	> 4200
Sylvia	1250	> 1250
Huberta	3000	1450 ± 40
Huberta	1100	920 ± 50
Hermione	3800	930 ± 10
Camilla	3800	1460 ± 50

each proper element. Fig. 11 displays the number of asteroids, simulated with the SYSYCE integrator, in the Huberta family region as a function of time (red line). We best-fitted a second-order polynomial to these data and extrapolated our results to 3 Gyr ago, the maximum possible age of the Huberta family as obtained with the method of the Yarkovsky isolines. The number of family members in that region will become less than 8, the minimum number of objects to identify a dynamical group, in 2.27 Gyr. We extrapolated that 3.00 Gyr ago the family may have had 80 members, assuming that the rate of population loss obtained from our simulations remained constant.

Our results are also summarized in Table 3, where for each family we show the time needed to have only eight members in the family region (dispersion time) for simulations with the $SWIFT - RMVSY$ and $SYSYCE$ integrators. As expected dispersions times obtained also considering the stochastic YORP effect tend to be higher than analogous times obtained with the simpler $SWIFT - RMVSY$ integrations, where no reorientations were considered (but timescales should be lower when compared with the dispersion times obtained with the static YORP effect, since the static YORP effect tends to change the shape, but not the orientation of the spin axis, Bottke et al. 2015). The dispersion time for the simulation with the stochastic YORP effect for the Sylvia family was slightly longer than the integration length and was computed extrapolating our results with the method described for the case of the Huberta family.

7.2   Past dynamical evolution

We then turned our attention to the past evolution of our studied families. For the two families for which it was possible to apply our Yarko-Yorp approach of Sect. 6, i.e., Sylvia and Huberta, we generated fictitious families with the ejection parameter V_{EJ} previously found and the number of objects the family that they were supposed to have at the

time of their formation. For the Huberta family, we extrapolated this number to the age estimated with the Yarko-Yorp method of Sect. 6, i.e. 1100 Myr, and for the maximum possible age obtained with the method of the Yarkovsky isolines, i.e., 3000 Myr. We obtained two families, with 48 and 80 members each. For the Sylvia family we extrapolated the number of objects to the time at which the family was formed according to the results of Sect. 6, i.e., 1220 Myr and $\simeq 1000$ members. Considering that information about the initial number of members of the possible oldest Sylvia family discussed in Sect. 6 is not easily available, we then also integrated the same family of 1000 members of the first Sylvia integration over the possible age of the first family, i.e., 4220 Myr. Since Bottke et al. (2012) suggested that the Late Heavy Bombardment may have started earlier than previously thought, with estimates as early as 4.1 Gyr ago (against the 3.8 Gyr previously assumed), this second age estimate of the Sylvia may possibly be in agreement with our new understanding of the LHB time of occurrence. As done in Sect. 6 for the Sylvia family, we also modified the $SYSYCE$ integrator to account for the lower past solar luminosity, according to Eq. 4. Finally, in view of the fact that Vokrouhlický et al. (2010) suggested that families around 107 Camilla and 121 Hermione could have formed in the past and then dispersed, we created fictitious families around these objects of 80 members each (the same estimated initial number of members of the Huberta family), and integrated these objects since 3800 Myr ago, i.e., after the most recent estimate for the end of the Late Heavy Bombardment (LHB). Because of the very small number of members of the Helga and Ulla group, we did not integrated these groups in the past, but in first approximation we can assume that dispersion times in the past for these groups should be of the same order of those obtained with integrations into the future.

Table 4 displays the dispersion times for our integrated families (third column), using the same box-like criteria discussed in Sect. 7.1. For the simulation with the Sylvia family over 1250 Myr, we found that the family was still detectable at the end of the run, with 104 objects in the Sylvia family region, thus confirming our previous estimate of Sect. 6.1. Extrapolating the current loss rates to the past, we estimated that the Sylvia family may have been $\simeq 7$ time more numerous at the time of its formation. At the end of the run
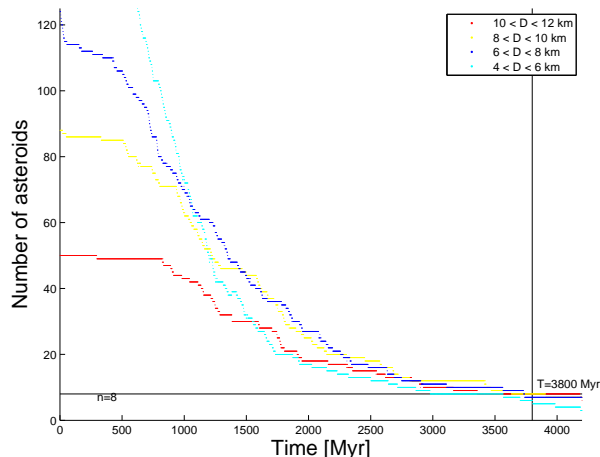
Figure 12. Number of Sylvia family members that remained in the Sylvia family region as a function of time. See the figure legend for the color code associated with each given range in particles diameter.

36.0% of the asteroids with $10 < D < 12$ km, 30.2% of those with $8 < D < 10$ km, and 18.5% of those with $6 < D < 8$ km were still in the Sylvia family region, so suggesting that only the largest fragments of an hypothetical LHB Sylvia family may still be visible today in the Cybele region. Of more interest were the results of the Sylvia simulations starting 4200 Myr ago.

In this longer simulation the Sylvia family did not completely dispersed up to the end at 4.2 Gyr. More importantly, 10.0% of the asteroids with $10 < D < 12$ km, 3.4% of those with $8 < D < 10$ km, 5.6% of those with $6 < D < 8$ km, and 0.8% of those with $4 < D < 6$ km could still be found at the end in the Sylvia family region. These results our displayed in Fig. 12, the horizontal black line shows the minimum number of objects to identify a cluster in the Cybele region (8), while the vertical black line shows the minimum estimated age for the end of the LHB (3.8 Gyr). See the figure legend for the color code associated with the each given range in particles diameter. As found in the shorter Sylvia simulation, we confirm that the largest fragments ($D > 7$ km) of a post-LHB Sylvia family could possibly remain in the Cybele region since its formation. We identify 30 X-type objects in this area with $p_v < 0.08$ and $D > 7$ km, two of which, (149776 and 172973), are current Sylvia family members. Since space weathering effects on X-type objects are not well understood (Nesvorný et al. 2005), the possibility that some of these asteroids predates the formation of the current Sylvia family remain speculative and difficult to prove. But, it could be an interesting field of future research. Finally, none of the simulated Sylvia fragments reached the regions of the Ulla and Helga families during the 4.2 Gyr simulations, which raises questions about the possible mechanisms that put the parent bodies of these groups in their current orbits.

Concerning the other integrated families, our results for the Huberta family seems to confirm the age estimate obtained in Sect. 6.2: in both the 1100 and 3000 Myr simulations the family dispersed in timescales comparable with the estimated age of the family, i.e., 1100 Myr. Extrapolating the current loss rates to the past, we estimated that the Huberta family may have been $\simeq 5$ time more numerous at the time of its formation. The upper estimate of the age of 3000 Myr would have required an initial population more than 10 times larger then the current one, which seems unlikely. Concerning the families proposed by Vokrouhlický et al. (2010), Camilla and Hermione, our results show that such families would have dispersed in timescales of the order of 1.5 Gyr at most. Should such families have formed before that time, they would no longer be recognizable, as suggested by these authors.

8 SYLVIA FAMILY DURING THE LATE HEAVY BOMBARDMENT

Since results in Sect. 7 suggested the possibility that some members of a pre-late heavy bombardment Sylvia family may have survived to the present, here we investigated what would have happened to a hypothetical family formed before $\simeq 4.0$ Gyr when Jupiter jumped in the jumping Jupiter scenario of planetary migration of Nesvorný et al. (2013). In this work the authors showed that the current orbital distribution of Jupiter Trojans may have occurred when Jupiter's orbit and its Lagrange points were displaced in a scattering event with an ice giant and felt into a region populated by planetesimal. Of the three models for this jump capture, we choose to work with their case 1, where five giant planets started in the 3:2, 3:2, 2:1, and 3:2 resonant chain, since this scenario was the most favourable in reproducing the current orbital distribution of Jupiter's Trojans.

To better understand the local dynamics before and after Jupiter jumped, we obtained dynamical maps in the $(a, sin(i))$ plane for the planetary configurations at the beginning and at the end of the 10 Myr integration with the scenario of Nesvorný et al. (2013). We integrated 4131 initially equally displaced particles in the $(a, sin(i))$ plane, in a grid of 51 by 81 particles, with a step in a of 0.01 AU and of $0.5°$ in i, starting from 3.20 AU and $0°$, respectively. The eccentricity and the other angles of the test particles were the same of 87 Sylvia at present. Fig. 13 displays our results for the two simulations. Black dots represent synthetic proper elements computed with the approach described in Sect. 2, while red vertical lines identify the positions of the main mean-motion resonances at each epoch. Mean-motion resonances appear as vertical strips deprived of particles, while secular resonances appears as inclined, low-density bands. Since timescales for migration are quite fast in the jumping Jupiter scenario, and of the order of the Myr, we ignored secular dynamics in this analysis. One can notice that the current Sylvia and Huberta families lie on top of the 2J:-1A mean-motions at the beginning of the scenario, and would have been destabilized on timescales of less then a few Myr. After Jupiter jumped, the 2J:-1A mean-motion resonance would have migrated towards smaller semi-major axis, but a series of three-body resonances currently at higher semi-major axis then the center of the 5J:-3A would also have been displaced inwards, making the Cybele region, and the Sylvia family region in particular, rather unstable. These results suggest that the Cybele asteroids should not be primordial, and must have reached their current orbits after Jupiter jumped.

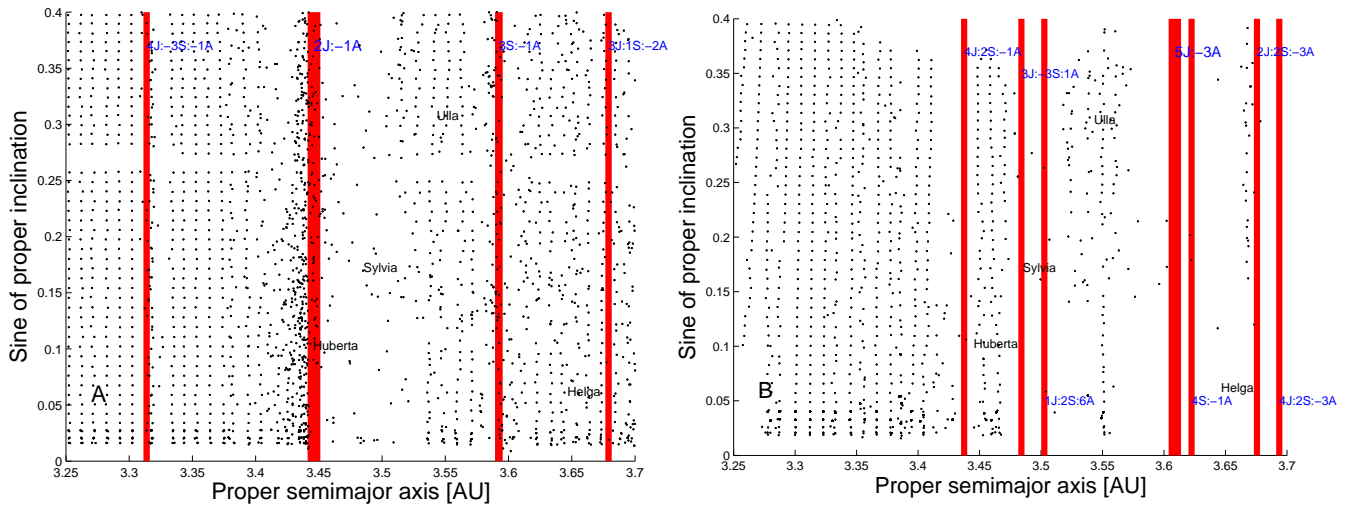To confirm the instabilities of asteroid families in the

Figure 13. A proper $(a, sin(i))$ map of test particles integrated under the influence of jovian planets before (panel A), and after (panel B) Jupiter jumped. Vertical red lines display the position of the main mean-motion resonances at each epoch.
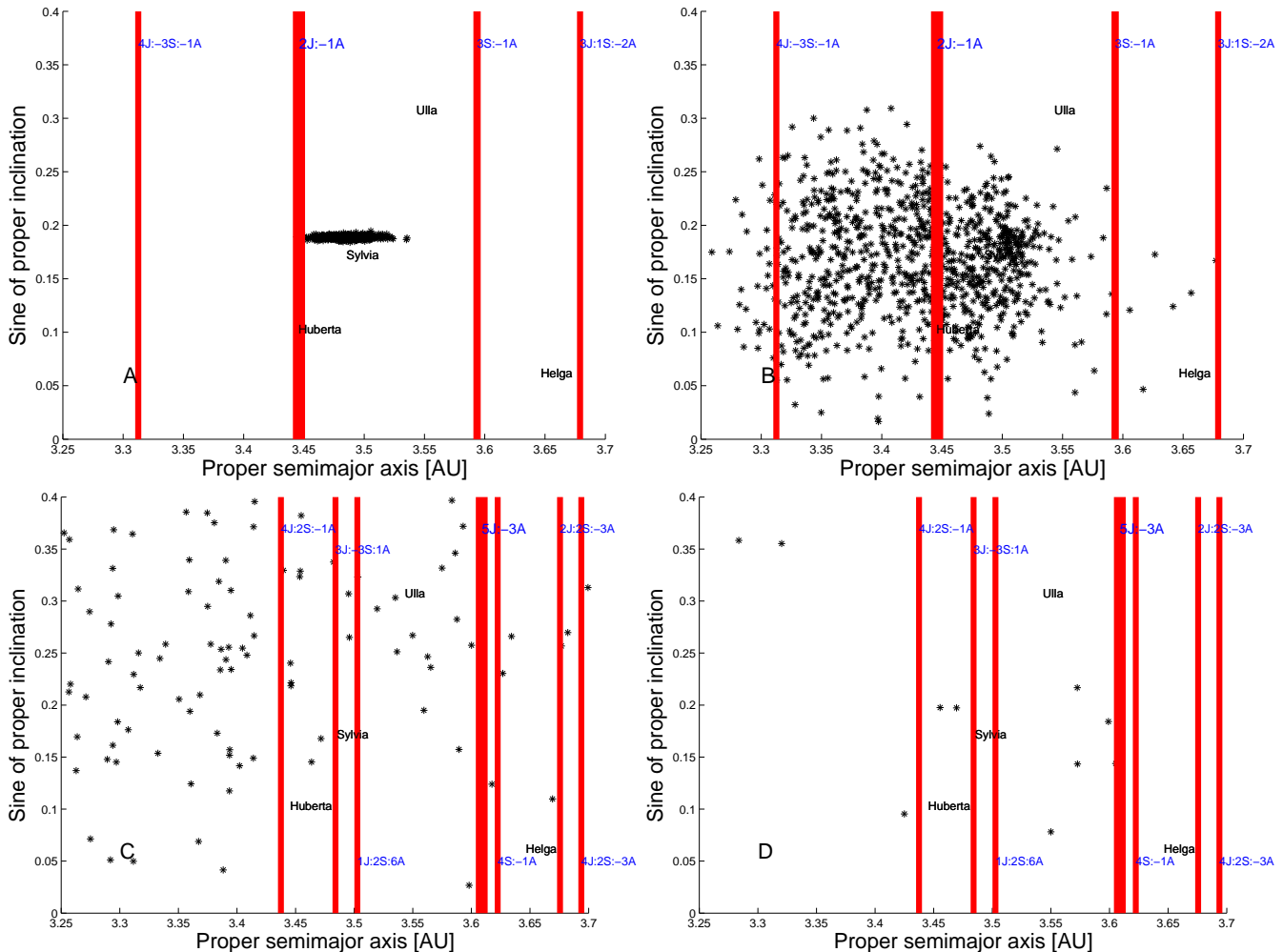

Figure 14. Panel A: an osculating $(a, sin(i))$ projection of asteroids at the beginning of the simulation with the case I of the jumping Jupiter model of Nesvorný et al. (2013). Vertical lines display the location of mean-motion resonances, as in Fig. 13, panel A. Panel B, C, and D: the same as panel A, but at t=5, 6, and 10 Myr, respectively. The instability occurred at 5.7 Myr. For panels C and D we show the location of mean-motion resonances after Jupiter jumped (see Fig. 13, panel B).

Cybele region with the jumping Jupiter scenario, we also integrated the same 1000 particles used for our simulation with the SYSYCE 4200 Myr integration of the Sylvia family discussed in Sect. 7.2, with the approach described in Nesvorný et al. (2013), Sect. 2, over 10 Myr. We choose to work with this timescales because this correspond to the period of planetary instability. In this scenario, Jupiter jumped at $t = 5.7$ Myr. Fig. 14 displays an osculating $(a, sin(i))$ projection of orbital elements of the integrated asteroids at the beginning (panel A), and at t =5, 6, and 10 Myr of the simulation. Since the particles osculating elements changed significantly over the length of the integration, we preferred not to compute proper elements in this case. Of the 1000 particles that were simulated in this scenario, only 7 had orbits in the Cybele orbital region at the end of our integration whose orbits were stable enough to allow the computation of synthetic proper element, i.e., 0.7% of the initial population. Overall, a pre-LHB Sylvia family would have been almost completely dispersed, so confirming the results of other authors for the Cybele region (Brož et al. 2013). Interestingly, 5 particles temporarily reached the Ulla family region during the length of the simulation, as defined in Sect. 7.2. Since Minton and Malhotra (2011) argued that the Ulla region should have been depopulated by the effect of sweeping secular resonances, and since we showed in Sect. 7.2 that the parent body of this family may have not reached its current orbit by mobility caused by the Yarkovsky and YORP effects, our results suggest that perhaps the Ulla family parent body could have been launched into its current orbit at the time when Jupiter jumped, either from regions at lower semi-major axis, as investigated in this paper, or, possibly, from the outer main belt. Investigating the second scenario is, in our opinion, beyond the purposes of this work, that aimed mostly at investigating the dynamics of Cybele asteroids. But it could be proposed as an interesting possible future line of research.

9 CONCLUSIONS

In this work we:

• Obtained high-quality synthetic proper elements for 1500 among numbered and multi-opposition asteroids in the Cybele region and computed the location of two-body and three-body mean-motion resonances using the approach of Gallardo (2014) for all resonances with a strength parameter R_S up to 10^{-5} for two-body and 10^{-4} for three-body resonances. As discussed in Gallardo (2014), the number density of mean-motion resonances grows considerably for semi-major axis larger than 3.7 AU.

• Studied the secular dynamics in the Cybele region and identified the population of librators currently in non-linear secular configurations. We identified a population of 32 asteroids in $g + s$-type secular resonances, 22 of which in z_1 librating configurations, so confirming the important role that this resonance has in shaping the dynamical evolution of asteroids in this region (see Vokrouhlický et al. 2010).

• Revised the information on physical properties (taxonomy, photometry, and geometric albedos) available in current spectroscopic surveys, SDSS-MOC4, and WISE data. As in Carruba et al. (2013), we found that the Cybele region is dominated by dark, low-albedo, primitive objects, with a

sizeable fraction of D-type bodies that were not detectable with the methods used in Carruba et al. (2013).

• We obtained dynamical families in the area using the Hierarchical Clustering Method of Zappalá et al. (1995), obtained a preliminary estimate of the family age using the method of the Yarkovsky isolines, and eliminated dynamical interlopers, objects with taxonomical properties consistent with those of other members of the family but whose current orbits current have been reached by dynamical evolution during the maximum estimated age of the family, using the approach of Carruba et al. (2014b). We identified the Sylvia, Huberta, and Ulla families of Nesvorný et al. (2015) and the Helga group of Vinogradova and Shor (2014), and confirmed the possibility that the Sylvia family might date from the last stages of planetary migration.

• Used the Monte Carlo approach of Vokrouhlický et al. (2006a, b, c), modified to account for the stochastic YORP effect of Bottke et al. (2015), and variability of the Solar luminosity, to obtain refined estimates of the Sylvia and Huberta family ages and ejection velocity parameter. Two possible family ages were obtained for the Sylvia family, $T = 1220 \pm 40\ Myr$, and $T = 4220^{+100}_{-120}\ Myr$, suggesting the possibility that multiple collisional events occurred on this asteroids. The Huberta family should be $T = 1100 \pm 50\ Myr$ old.

• Investigated the past and future dynamical evolution of the Sylvia, Huberta, and of the possibly currently depleted families of Camilla and Hermione using newly developed symplectic integrators that simulates both the stochastic YORP effect and variability of the Solar luminosity. We confirmed the age estimates for our families found with previous methods and found that a fraction of about 5% of the largest fragments of a hypothetical Sylvia family that formed just after the LHB could have remained in the Cybele region up to these days (but would be of difficult identification). Any family that formed from the binary asteroids Camilla and Hermione should have dispersed in time-scale of 1.5 Gyr at most, in agreement with previous results (Vokrouhlický et al., 2010).

• Studied the dynamical evolution of a fictitious Sylvia family formed before Jupiter jumped in the jumping Jupiter scenario of planetary migration, case I, of Nesvorný et al. (2013). As suggested by other authors (Brož et al. 2013), such family would have been most likely dispersed beyond recognition, with only a handful of members surviving in the Cybele orbital region. We propose that the parent body of the Ulla family may have been scattered to its current orbit during this phase of planetary migration.

Overall, our analysis seems to be in agreement with that of previous works: we confirm, with some caveats, the possible existence of the Helga group of Vinogradova and Shor (2014), we confirmed that the Sylvia family should be at least 1 Gyr old, with some of its members possibly coming from previous, no longer detectable dynamical families. Families that formed from the binaries Camilla and Hermione should have dispersed on timescales of 1.5 Gyr at most (see also Vokrouhlický et al., 2010). Finally, any dynamical group that predated the LHB in the Cybele region was most likely dispersed when Jupiter jumped. The possible identification of X-type asteroids in the Cybele region that formed in possible collisional event that predated the

formation of the current Sylvia family remains a challenge for future works.

REFERENCES

Beaugé, C., Roig, F., 2001, Icarus, 153, 391.

Bottke, W. F., and 7 co-authors, 2012, Nature, 485, 78.

Bottke, W. F., and 10 co-authors, 2014, Icarus, 247, 191.

Brož, M., 1999, Thesis, Charles Univ., Prague, Czech Republic.

Brož, M., Morbidelli, A., Bottke, W. F., Rozenhal, J., Vokrouhlický, D, and Nesvorný, D. 2013, A&A, 551, A117.

Čapek, D., and Vokrouhlický, D., 2004, Icarus, 172, 526.

Carruba V., Burns, J. A., Bottke, W., Nesvorný, D. 2003, Icarus, 162, 308.

Carruba, V., Roig, F., Michtchenko, T., Ferraz-Mello, S., and Nesvorný, D. 2007. A&A 465, 315.

Carruba, V., 2009a, MNRAS, 395, 358.

Carruba, V., 2010b, MNRAS, 408, 580.

Carruba, V., Domingos, R. C., Nesvorný, D., Roig, F., Huaman, M. E.,Souami D., 2013, MNRAS, 433, 2075.

Carruba, V., Domingos, R. C., Huaman, M. E., Dos Santos, C. R., Souami D., 2014a, MNRAS, 437, 2279.

Carruba, V., Aljbaae, S., Souami, D. 2014b, APJ, 792, 46.

Carry, B., 2012, Planet. Spa. Sci., 73, 98.

DeMeo, F., Carry, B., 2013, Icarus, 226, 723.

Gallardo, T. 2014, Icarus, 231, 273.

Ivezić, Ž, and 34 co-authors, 2001, AJ, 122, 2749.

Knežević, Z., Milani, A., 2003, A&A, 403, 1165.

Milani, A., Nobili, A.-M. 1985, A&A, 144, 261.

Milani, A., Nobili, A.-M. 1992, Nature, 357, 569.

Milani, A., Nobili, A.-M. 1993, CMDA 56, 323.

Milani, A., Cellino, A., Knežević, Z., 2014. Icarus, 239, 46.

Minton, D., Malhotra, R., APJ, 732, 53.

Masiero, J. R., Mainzer, A. K., Grav, T., Bauer, J. M., and Jedicke, R., 2012, APJ, 759, 14.

Nesvorný, D., Jedicke, R., Whiteley, R. J., Ivezić, Z., 2005, Icarus, 173, 132.

Nesvorný, D., Vokrouhlický, D., Morbidelli, A., 2013, APJ, 768, 45.

D. Nesvorný, M. Brož, V. Carruba 2015, Identification and Dynamical Properties of Asteroid Families. In Asteroid IV, (P. Michel, F. E.De Meo, W. Bottke Eds.), Univ. Arizona Press and LPI, in press.

Press, V.H., Teukolsky, S. A., Vetterlink, W. T., Flannery, B. P., 2001, Numerical Recipes in Fortran 77, Cambridge Univ. Press, Cambridge.

Pravec, P., Vokrouhlický D., 2009, Icarus, 216, 69.

Vinogradova, T., Shor, V., 2014, Proceedings of Asteroids, Comets and Meteors 2014, Helsinki, Finland.

Vokrouhlický, D., Brož, M., Morbidelli, A., et al. 2006a, Icarus, 182, 92.

Vokrouhlický D., Brož, M., Bottke, W. F., Nesvorný, D., Morbidelli, A. 2006b, Icarus, 182, 118.

Vokrouhlický D., Brož, M., Bottke, W. F., Nesvorný, D., Morbidelli, A. 2006c, Icarus, 183, 349.

Vokrouhlický, Nesvorný, D., Bottke, W. F., Morbidelli, A. 2010, AJ, 139, 2148.

Zappalà V., Cellino, A., Farinella, P., Knežević, Z. 1990, AJ, 100, 2030.

Zappalà, V., Bendjoya, Ph., Cellino, A., Farinella, P., Froeschlé, C., 1995, Icarus, 116, 291.

This paper has been typeset from a TeX/ LaTeX file prepared by the author.